



## Weak Localization of Light in Superdiffusive Random Systems

Matteo Burrelli,<sup>1,2,\*</sup> Vivekananthan Radhalakshmi,<sup>1,3</sup> Romolo Savo,<sup>1,3</sup> Jacopo Bertolotti,<sup>3,4</sup>  
Kevin Vynck,<sup>1,3,†</sup> and Diederik S. Wiersma<sup>1,2</sup>

<sup>1</sup>European Laboratory for Non-linear Spectroscopy (LENS), 50019 Sesto Fiorentino (FI), Italy

<sup>2</sup>Istituto Nazionale di Ottica (CNR-INO), Largo Fermi 6, 50125 Firenze (FI), Italy

<sup>3</sup>Dipartimento di Fisica e Astronomia, Università di Firenze, 50019 Sesto Fiorentino (FI), Italy

<sup>4</sup>MESA+ Institute for Nanotechnology, University of Twente, 7500 AE Enschede, The Netherlands

(Received 7 October 2011; published 15 March 2012; corrected 23 March 2012)

Lévy flights constitute a broad class of random walks that occur in many fields of research, from biology to economy and geophysics. The recent advent of Lévy glasses allows us to study Lévy flights—and the resultant superdiffusion—using light waves. This raises several questions about the influence of interference on superdiffusive transport. Superdiffusive structures have the extraordinary property that all points are connected via direct jumps, which is expected to have a strong impact on interference effects such as weak and strong localization. Here we report on the experimental observation of weak localization in Lévy glasses and compare our results with a recently developed theory for multiple scattering in superdiffusive media. Experimental results are in good agreement with theory and allow us to unveil the light propagation inside a finite-size superdiffusive system.

DOI: 10.1103/PhysRevLett.108.110604

PACS numbers: 05.40.Fb, 05.60.-k, 42.25.Dd

Lévy flights define a general class of random walks, lying beyond the commonly known Brownian motion, for which the distribution of step lengths has a diverging variance [1,2]. Random walks based on Lévy statistics [3,4] are dominated by a few very long steps, thereby leading to a transport process called superdiffusion, for which the mean square displacement increases faster than linear in time [5,6]. Lévy processes are common in nature and appear, for instance, in animal foraging [7,8], laser cooling of cold atoms [9], evolution of the stock market [10], astronomy [11], random lasers [12], and turbulent flow [13].

Random optical materials provide an excellent test bed to study complex transport phenomena, due to the broad scale of available optical characterization techniques. The experimental realization of a Lévy walk and superdiffusion is, however, not easy since it requires creating the appropriate step-length distribution over a broad range of length scales. Very interesting in this respect are the so-called fractal aggregates of microscopic particles, obtained by preparing suspensions of microspheres that in certain conditions cluster and give rise to agglomerations with a fractal structure [14,15]. The disadvantage of such structures is that their fractal behavior extends only over a limit length scale and their distribution is difficult to control. The recent development of Lévy glasses [16] and hot atomic vapors [17] has allowed the observation of Lévy flights of light waves and the resulting superdiffusion process. Recent works have modeled incoherent light transport in Lévy-type systems [18–20]. Since interference effects play a dominant role in light transport [21], this raises the natural question of how interference influences optical superdiffusion—a concept which has not been addressed so far.

Among all interference phenomena in random optical materials, maybe the most robust is that of weak localization [21]. It is observed in the form of a cone of enhanced backscattering, which contains information on the path length distribution deep inside the random system and which has been observed in recent years from several diffusive random structures [22–27]. In one of the first extensive theoretical studies of weak localization, the case of anomalous transport—beyond regular diffusion—was discussed, in particular, for a random walk on a fractal [28]. More recently, it was shown how the generally used diffusion approximation in multiple light scattering theory can be expanded to superdiffusion and what consequences this has for weak localization [29].

In this Letter we report on the experimental observation of weak localization from superdiffusive materials, which constitutes the first observation of an interference effect in transport based on Lévy statistics. We find a good agreement with superdiffusive transport theory and show how the backscattering cone can be used to extract the Green's function in a Lévy glass. Contrary to regular diffusive media, in a Lévy glass, light from an *arbitrary* depth inside the medium has a nonvanishing probability to couple directly to the surrounding environment. This latter property makes light scattering from Lévy glasses complex, and has important consequences for its (back)scattering properties.

The Lévy glasses under investigation are made of jammed microscopic glass spheres, whose diameter ( $\phi$ ) varies almost over 2 order of magnitude (from 5 to 230  $\mu\text{m}$ ) following a power-law distribution  $p(\phi) \sim \phi^{-(\beta+1)}$ , with  $\beta$  adjustable parameter. These spheres are embedded in a polymeric matrix which matches their refractive index ( $n = 1.52$ ) and in which  $\text{TiO}_2$

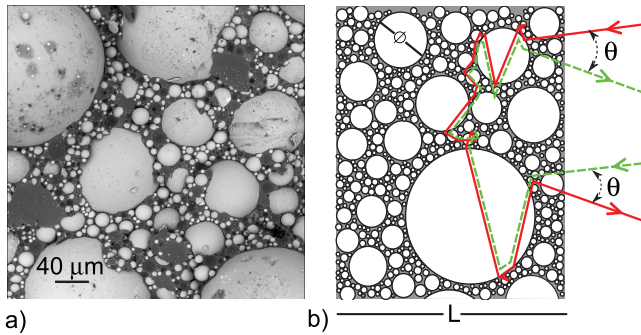


FIG. 1 (color). (a) Electron micrograph of the interior of a Lévy glass. (b) Sketch representing the optical mechanism lying behind the coherent backscattering cone in a Lévy glass.  $L = 300 \mu\text{m}$  is the thickness of the sample and  $\phi$  the diameter of the spheres. In both images the scale invariance of the system is evident.

nanoparticles (average diameter 280 nm) have been dispersed [Fig. 1(a)] [30]. Because their refractive index ( $n = 2.4$ ) is higher than the polymer, these nanoparticles act as point scatterers which are not homogeneously distributed throughout the sample due to the presence of the glass spheres [Fig. 1(b)]. As a result, light transport is dominated by the long “jumps” that light performs propagating through the microscopic spheres. The step-length distribution that light performs in Lévy glasses follows a power-law decay as  $p(l) \sim l^{-(\alpha+1)}$ , where  $\alpha$  is related to  $\beta$  as  $\alpha = \beta - 1$  for an exponential sampling of the diameter distribution [30]. In practice, the step-length distribution is truncated by the diameter of the largest sphere.

By controlling the diameter distribution of the spheres in a Lévy glass we can control  $\alpha$  and, thus, the degree of superdiffusion of the material. For  $\alpha \geq 2$  the system is diffusive, whereas for  $0 < \alpha < 2$  the system is superdiffusive. In real finite systems the truncation of the step-length distribution leads to a transition from superdiffusion to diffusion [18,19]. In previous publications [16,30] Lévy glasses were fabricated between two microscope slides. In this work we remove one of the two slides to reduce undesirable reflections which affect the quality of the measurements. Moreover, the thickness of the sample is

approximately  $70 \mu\text{m}$  more than the largest sphere, to avoid direct reflections from the microscope slide on the back of the sample. This means that the sample is slightly thicker than the cutoff length of the step-length distribution. We found that this increased thickness does not significantly influence the shape of the backscattering cone within the accuracy of our measurements.

The setup employed follows a common scheme for coherent backscattering experiments. Light emitted by a HeNe laser (at 632 nm) is expanded to a collimated beam of about 1 cm in diameter to ensure a high angular resolution of the system. A beam splitter is used to separate the backscattered light from light impinging on the sample. Subsequently, the backscattering cone is imaged on a CCD camera and the use of a polarizer ensures that we observe only the polarization conserving channel [21]. The sample is nutated to average over different disorder realizations.

We measured the backscattering cone on two different sets of superdiffusive samples characterized by  $\alpha = 1.5$  and  $\alpha = 1$ , and reference samples made of  $\text{TiO}_2$  and polymer (without glass spheres). In the reference samples the concentration of  $\text{TiO}_2$  was chosen to obtain the same overall density of scatterers as in the superdiffusive samples. The experimental results are shown in Fig. 2, together with a fit to diffusion theory (red line) [24]. While in the case of the diffusive sample there is a perfect match between experiment and theory ( $\ell^* \approx 19 \mu\text{m}$ ), in the superdiffusive case in Figs. 2(b) and 2(c) it is clear that regular diffusion theory cannot properly describe the optical properties of Lévy glasses. In particular, one can notice the rising of the tail of the cone as the degree of superdiffusion increases, i.e., when  $\alpha$  decreases.

The coherent backscattering cone for the superdiffusive samples under investigation can be calculated by taking advantage of the fractional derivative approach developed in Ref. [29], which allows us to take into account the finite sample size and cutoff in the path length distribution. The transport of light in a finite, in-plane translationally invariant, superdiffusive system for a point source at  $x_0$  is described by the stationary fractional diffusion equation [29]:

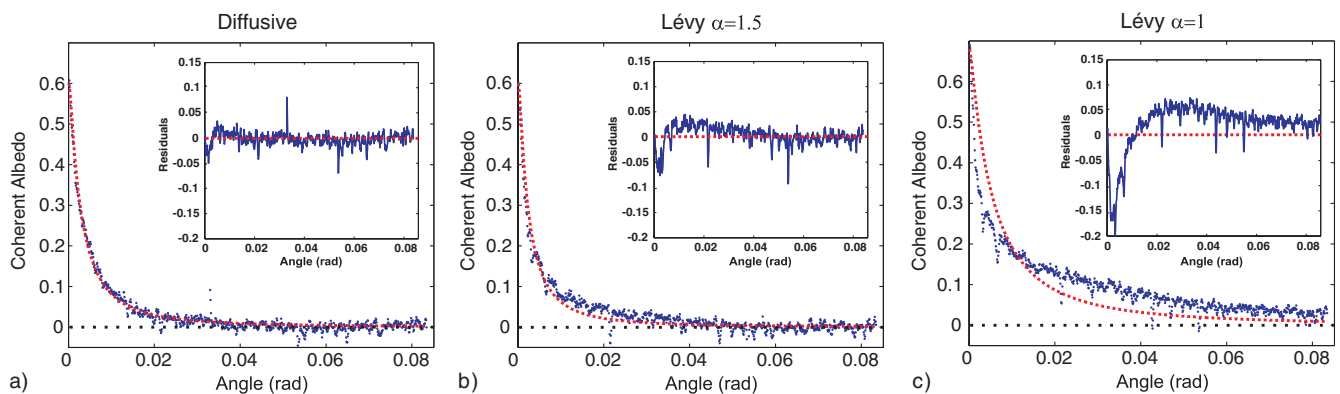


FIG. 2 (color). (a)–(c) Measured coherent backscattering cone from diffusive samples and Lévy glasses with  $\alpha = 1.5$  and  $\alpha = 1$ , respectively. In red, fit to the experimental data according to standard diffusion theory. Insets: Residuals of the fits.

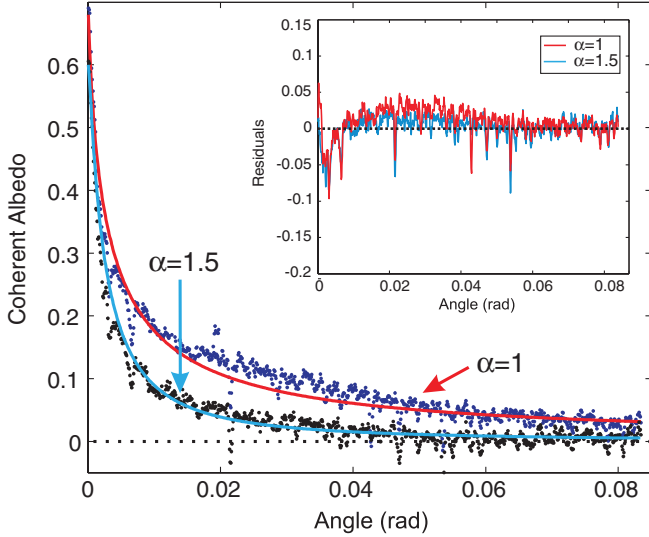


FIG. 3 (color). Comparison between the calculated superdiffusive cones obtained with the fractional derivative approach and the measured Lévy cones (blue for  $\alpha = 1$ , red for  $\alpha = 1.5$ ).

$$D_\alpha(\nabla_z^\alpha - k_\perp^\alpha)f(z, z_0, \mathbf{k}_\perp) = -\delta(z - z_0), \quad (1)$$

where  $\nabla^\alpha$  is the symmetric Riesz fractional derivative with respect to spatial derivatives,  $\mathbf{k}_\perp$  is the in-plane component of the wave vector in free space,  $f(z, z_0, \mathbf{k}_\perp)$  is the intensity propagator, and  $D_\alpha$  is a generalized diffusion constant. The spatial nonlocality of  $\nabla^\alpha$  makes the definition of boundary conditions nontrivial [31]. In order to model physical systems, such as Lévy glasses, the fractional Laplacian operator can be represented by an  $M \times M$  matrix, whose eigenvalues  $\lambda_i$ , rescaled as  $\lambda_i \rightarrow \lambda_i(M/L)^\alpha$  with  $L$  the slab thickness, and eigenvectors  $\psi_i$  converge to those of the continuum operator as  $M$  goes to infinity [32]. Absorbing boundary conditions can be implemented by reducing the infinite size matrix to a finite-size matrix and Eq. (1) can be solved by eigenfunction expansion. The knowledge of the intensity propagator of the system then makes it possible to calculate interference effects in a *superdiffusion*

approximation. In particular, considering a plane wave at normal incidence on the slab interface and in the Fraunhofer regime, the coherent component of the albedo is given by the following expression:

$$A_c(\theta) \propto - \sum_{z_1, z_2} F(z_1, z_2, \theta) \sum_{i=1}^M \frac{\psi_i(z_1)\psi_i(z_2)}{(\lambda_i - k_\perp^\alpha)}, \quad (2)$$

where  $F(z_1, z_2, \theta) = P(z_1)P(z_2)P(z_1/\cos\theta)P(z_2/\cos\theta)$  describes the attenuation for the amplitude of the incident and emergent plane waves in the scattering medium,  $\theta$  is the angle between the incident and emergent plane waves [Fig. 1(b)], and  $k_\perp = |\mathbf{k}_\perp| \simeq (2\pi/\lambda)\theta$ , at small angle  $\theta$ . The amplitude attenuation  $P(l)$  is modeled as a Pareto-like distribution  $P(l) = 1$  for  $0 \leq l \leq l_c$  and  $P(l) = (l_c/l)^{(\alpha+1)/2}$  for  $l \geq l_c$ , where  $l_c$  is the cutoff length, as to closely follow the step-length distribution of real Lévy glasses [18]. Internal reflections are neglected.

The results are shown in Fig. 3 for  $\alpha = 1.5$  and  $\alpha = 1$ , where the *only* adjustable parameter used is  $l_c$ . The inset shows the residuals between theory and experiment, which are greatly reduced with respect to the diffusive fit [Figs. 2(b) and 2(c)]. Because of the very long tail of the cones for Lévy glasses and the lack of an analytical expression for it, the experimental incoherent background is set to the one obtained semianalytically. It must be pointed out that for these calculations we employed a step-length distribution which was not truncated, in contrast to the real system. This is due to the fact that the propagator  $f(z, z_0, \mathbf{k}_\perp)$  of the system has been calculated by considering the sample as translational invariant in the in-plane direction and finite in the longitudinal direction. A transition in the shape of the cone due to the truncation is expected to manifest itself mostly at small angles, which are below the resolution of our setup. The very good agreement between experiment and calculation shows that the fractional diffusion approach can properly describe light interference effects due to multiple scattering in the superdiffusion approximation.

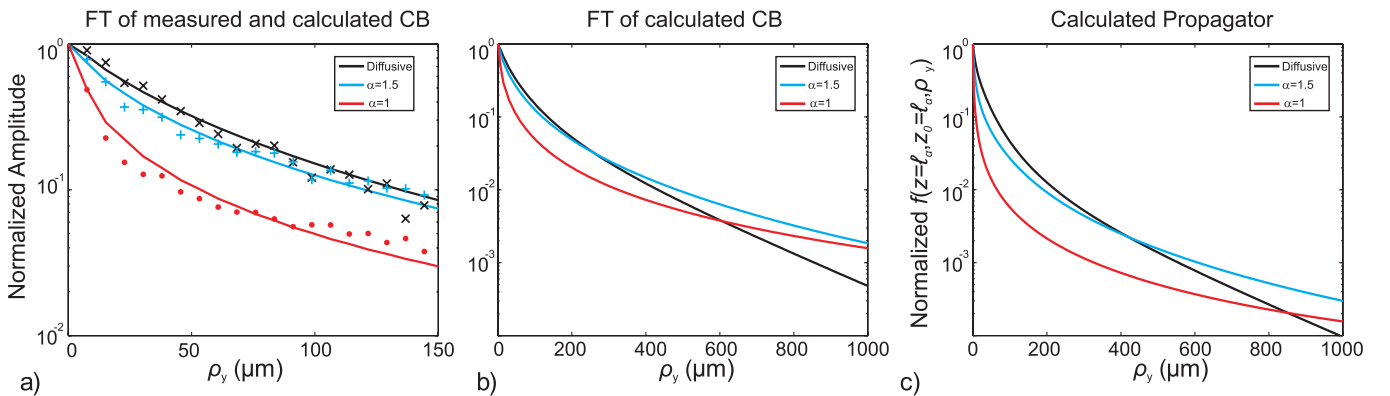


FIG. 4 (color). (a) Amplitude of the Fourier transform (FT) of the measured and calculated coherent backscattering (CB) for small  $\rho_y$ . (b),(c) Amplitude of the Fourier transform of the calculated CB and intensity distribution  $f(x = \ell_\alpha, z_0 = \ell_\alpha, \rho_y)$  for large  $\rho_y$ .

The characteristic features of the backscattering cone taken from a Lévy glass include a sharpening of the top and at the same time a more gentle decay at large angles, leading to an apparent broadening of the cone with decreasing  $\alpha$ . At first sight this might be counterintuitive, since the width is expected to be inversely proportional to the mean free path  $\ell$ , whereas in a Lévy glass the average step length  $\ell_\alpha$  increases when  $\alpha$  decreases. An analysis of the Green's function can help to shed light on this behavior. The backscattering cone is basically the Fourier transform of the lateral intensity distribution created by a point source inside the medium [33]. The propagator can therefore be well approximated by performing a Fourier analysis of the experimentally observed coherent backscattering.

In Fig. 4(a) the normalized Fourier transform of the measured and calculated coherent albedo as a function of the displacement along the in-plane  $y$  direction  $\rho_y = |(\mathbf{r}_1 - \mathbf{r}_2)_y|$  are shown. These curves are found to be in good agreement and show a remarkable reshaping as a function of  $\alpha$ . In Figs. 4(b) and 4(c) the normalized Fourier transform of the theoretical cone and the normalized intensity distribution  $f(z = \ell_\alpha, z_0 = \ell_\alpha, \rho_y)$  calculated from the fractional diffusion approach for an ideal (untruncated) Lévy walk in a slab, respectively, are shown for long  $\rho_y$ . The qualitative agreement between these two figures is evident, in particular, in their dependency on the degree of superdiffusion. The spatial distribution of the propagator is dictated by the power-law step-length distribution in Lévy glasses, which allows light to couple directly to the surrounding environment from *any* depth inside the sample. This spatial nonlocality applied to an open system such as a Lévy glass results in a strong modification of the shape of the propagator as a function of  $\alpha$  [29]. The fact that light can escape more easily from its local environment towards large distances makes the cusp of  $f(z = \ell_\alpha, z_0 = \ell_\alpha, \rho_y)$  sharper, giving rise to slowly decaying tails in the coherent albedo, while the gentle tail of  $f(z = \ell_\alpha, z_0 = \ell_\alpha, \rho_y)$ , due to the very long trajectories, results in a sharper cusp for the coherent albedo. It would be interesting to look into the effect of such long-range behavior in strongly scattering systems close to or in the Anderson localized regime, where superdiffusion would most likely counteract localization to a certain extent. It is also likely that the critical dimension above which a localization transition occurs reduces from 2 to a value related to  $\alpha$ . Vice versa, around the localization transition, diffusion can become anomalous due to a size and distance dependence renormalization of the diffusion constant [34–36].

We wish to thank R. Burioni, A. Vezzani, S. Lepri, and R. Livi for fruitful discussions. This work is supported by the European Network of Excellence Nanophotonics for Energy Efficiency, CNR-EFOR, ENI S.p.A. Novara, and the Italian FIRB-MIUR “Futuro in Ricerca” Project No. RBFR08UH60.

\*burrese@lens.unifi.it

†vynck@lens.unifi.it

- [1] B. Mandelbrot, *The Fractal Geometry of Nature* (W. H. Freeman, San Francisco, 1977).
- [2] M. F. Shlesinger, G. M. Zaslavsky, and J. Klafter, *Nature (London)* **363**, 31 (1993).
- [3] P. Lévy, *Theorie de l'addition des Variables Aleatoires* (Gauthier-Villars, Paris, 1954).
- [4] J. P. Nolan, *Stable Distributions* (Birkhauser, Boston, 2002).
- [5] P. M. Drysdale and P. A. Robinson, *Phys. Rev. E* **58**, 5382 (1998).
- [6] R. Metzler and J. Klafter, *Phys. Rep.* **339**, 1 (2000).
- [7] G. M. Viswanathan *et al.*, *Nature (London)* **401**, 911 (1999).
- [8] F. Bartumeus *et al.*, *Ecology* **86**, 3078 (2005).
- [9] F. Bardou *et al.*, *Phys. Rev. Lett.* **72**, 203 (1994).
- [10] B. Mandelbrot, *J. Bus.* **36**, 394 (1963).
- [11] S. Boldyrev and C. R. Gwinn, *Phys. Rev. Lett.* **91**, 131101 (2003).
- [12] D. Sharma, H. Ramachandran, and N. Kumar, *Opt. Lett.* **31**, 1806 (2006).
- [13] T. H. Solomon, E. R. Weeks, and H. L. Swinney, *Phys. Rev. Lett.* **71**, 3975 (1993).
- [14] A. Dogariu and T. Asakura, *Opt. Rev.* **3**, 71 (1996).
- [15] K. Ishii and T. Iwai, *J. Opt. A* **2**, 505 (2000).
- [16] P. Barthelemy, J. Bertolotti, and D. S. Wiersma, *Nature (London)* **453**, 495 (2008).
- [17] N. Mercadier *et al.*, *Nature Phys.* **5**, 602 (2009).
- [18] P. Barthelemy *et al.*, *Phys. Rev. E* **82**, 011101 (2010).
- [19] C. W. Groth, A. R. Akhmerov, and C. W. J. Beenakker, *Phys. Rev. E* **85**, 021138 (2012).
- [20] P. Buonsante, R. Burioni, and A. Vezzani, *Phys. Rev. E* **84**, 021105 (2011).
- [21] E. Akkermans and G. Montambaux, *Mesoscopic Physics of Electrons and Photons* (Cambridge University Press, Cambridge, England, 2007).
- [22] Y. Kuga and A. Ishimaru, *J. Opt. Soc. Am. A* **1**, 831 (1984).
- [23] M. P. Van Albada and A. Lagendijk, *Phys. Rev. Lett.* **55**, 2692 (1985); P. E. Wolf and G. Maret, *Phys. Rev. Lett.* **55**, 2696 (1985).
- [24] D. S. Wiersma, M. P. van Albada, and A. Lagendijk, *Phys. Rev. Lett.* **75**, 1739 (1995).
- [25] G. Labeyrie *et al.*, *Phys. Rev. Lett.* **83**, 5266 (1999).
- [26] R. Sapienza *et al.*, *Phys. Rev. Lett.* **92**, 033903 (2004).
- [27] M. Gurioli *et al.*, *Phys. Rev. Lett.* **94**, 183901 (2005).
- [28] E. Akkermans, P. E. Wolf, R. Maynard, and G. Maret, *J. Phys. (Paris)* **49**, 77 (1988).
- [29] J. Bertolotti, K. Vynck, and D. S. Wiersma, *Phys. Rev. Lett.* **105**, 163902 (2010).
- [30] J. Bertolotti *et al.*, *Adv. Funct. Mater.* **20**, 965 (2010).
- [31] A. V. Chechkin *et al.*, *J. Phys. A* **36**, L537 (2003).
- [32] A. Zoia, A. Rosso, and M. Kardar, *Phys. Rev. E* **76**, 021116 (2007).
- [33] E. Akkermans, P. E. Wolf, and R. Maynard, *Phys. Rev. Lett.* **56**, 1471 (1986).
- [34] R. Berkovits and M. Kaveh, *Phys. Rev. B* **36**, 9322 (1987).
- [35] I. Edrei and M. J. Stephen, *Phys. Rev. B* **42**, 110 (1990).
- [36] F. J. P. Schuurmans *et al.*, *Phys. Rev. Lett.* **83**, 2183 (1999).